

EPR Spectroscopy of Nitrite Complexes of Methemoglobin

David E. Schwab[†]

Department of Chemistry and Biochemistry, Montana State University, P.O. Box 173400, Bozeman, Montana 59717

Jonathan S. Stamler[‡]

Department of Medicine, Duke University Medical Center, Box 2612, Durham, North Carolina 27710

David J. Singel^{*}

Department of Chemistry and Biochemistry, Montana State University, P.O. Box 173400, Bozeman, Montana 59717. [†] E-mail: deschwab@chemistry.montana.edu. [‡] E-mail: staml001@mc.duke.edu.

Received October 21, 2009

The chemical interplay of nitrogen oxides (NO's) with hemoglobin (Hb) has attracted considerable recent attention because of its potential significance in the mechanism of NO-related vasoactivity regulated by Hb. An important theme of this interplay—redox coupling in adducts of heme iron and NO's—has sparked renewed interest in fundamental studies of FeNO_x coordination complexes. In this Article, we report combined UV–vis and comprehensive electron paramagnetic resonance (EPR) spectroscopic studies that address intriguing questions raised in recent studies of the structure and affinity of the nitrite ligand in complexes with Fe^{III} in methemoglobin (metHb). EPR spectra of metHb/NO₂[−] are found to exhibit a characteristic doubling in their sharper spectral features. Comparative EPR measurements at X- and S-band frequencies, and in D₂O versus H₂O, argue against the assignment of this splitting as hyperfine structure. Correlated changes in the EPR spectra with pH enable complete assignment of the spectrum as deriving from the overlap of two low-spin species with *g* values of 3.018, 2.122, 1.45 and 2.870, 2.304, 1.45 (values for samples at 20 K and pH 7.4 in phosphate-buffered saline). These *g* values are typical of *g* values found for other heme proteins with N-coordinated ligands in the binding pocket and are thus suggestive of N-nitro versus O-nitrito coordination. The positions and shapes of the spectral lines vary only slightly with temperature until motional averaging ensues at ~150 K. The pattern of motional averaging in the variable-temperature EPR spectra and EPR studies of Fe^{III}NO₂[−]/Fe^{II}NO hybrids suggest that one of two species is present in both of the α and β subunits, while the other is exclusive to the β subunit. Our results also reconfirm that the affinity of nitrite for metHb is of millimolar magnitude, thereby making a direct role for nitrite in physiological hypoxic vasodilation difficult to justify.

Introduction

The chemical interaction of nitrite with hemoglobin (Hb) has attracted considerable recent attention because of its potential significance in the mechanism of nitrogen oxide (NO)-related vasoactivity regulated by Hb, namely, hypoxic vasodilation. While the specific nature of nitrite's possible roles in this physiological process has been debated, the critical assessment of all of the available data, recently published by Allen et al.,¹ consolidates the view that the central signaling entity in hypoxic vasodilation is the S-nitroso derivative of Hb, SNO-Hb, which has the unique capacity to

effect a prompt NO-dependent modulation of blood flow in response to Hb oxygen saturation over physiological oxygen gradients, as red blood cells (RBCs) pass from arterial to venous circulation. This assessment allows only an indirect, albeit potentially important, role for nitrite, which, for example, could, through slower biochemical pathways, raise stores of SNO-Hb.

Luchsinger et al.^{2,3} had already, in 2003, used the well-known reaction of nitrite with deoxyhemoglobin (deoxyHb) to produce SNO-Hb and thus to exemplify one of several

^{*}To whom correspondence should be addressed. E-mail: dsingel@chemistry.montana.edu. Tel.: 406-994-3960.

(1) Allen, B. W.; Stamler, J. S.; Piantadosi, C. A. *Trends Mol. Med.* **2009**, *15*, 452–460.

(2) Luchsinger, B. P.; Rich, E. N.; Gow, A. J.; Williams, E. M.; Stamler, J. S.; Singel, D. J. *Proc. Natl. Acad. Sci. U.S.A.* **2003**, *100*, 461–466.

(3) McMahon, T. J.; Moon, R. E.; Luchsinger, B. P.; Carraway, M. S.; Stone, A. E.; Stolp, B. W.; Gow, A. J.; Pawloski, J. R.; Watke, P.; Singel, D. J.; Piantadosi, C. A.; Stamler, J. S. *Nat. Med.* **2002**, *8*, 711–7.

routes of SNO-Hb synthesis that involve redox coupling of heme iron and NO to support nitrosative chemistry. This work brought increased attention to the role of Fe^{II}-containing met-hemes and their complexes with NO's in such transformations^{4–6} and prompted renewed interest in the spectroscopic characterization of such complexes to facilitate analysis of this chemistry.

This interest was further piqued recently by the report of Basu et al.,⁶ who measured the affinity of methemoglobin (metHb) for nitrite by an indirect electron paramagnetic resonance (EPR) technique. Specifically, they monitored the progressive loss of the high-spin metHb EPR signal with successive additions of nitrite and, assuming a simple equilibrium, determined a substantially higher affinity than was previously determined by UV–vis spectroscopy.⁷ Intriguingly, they did not detect the EPR spectrum of the complex, an outcome that was surprising, inasmuch as EPR spectra have been previously reported both for low-spin nitrite complexes with metmyoglobin, and for RBCs treated with nitrite.⁹ We therefore undertook a reinvestigation of the EPR spectroscopy of the nitrite/metHb complex. We were able to elicit the expected nitrite/metHb spectrum, to demonstrate, through mass balance, that it was essentially the sole reaction product and, by quantitative analysis of both the protein reactant and product, to determine an affinity in agreement with the previous studies that had been questioned by Basu et al. These findings were reported in a brief account published elsewhere.¹⁰

The observed EPR spectra exhibited a distinct structure—a doubling of certain spectral features—that motivated further study. This motivation is enhanced by recent X-ray crystallographic studies that have demonstrated structural and linkage isomerization in nitrite coordination to metHb¹¹ and thus raise the possibility that the spectral features might arise from structurally distinct coordination complexes. Here we report a comprehensive EPR study of the nitrite/metHb complex, in which we test different possible origins of the spectral structure. We also elaborate our previous brief remarks¹⁰ on evidence for the weak affinity between metHb and the nitrite ligand.

Materials and Methods

Hemoglobin (Hb). Hb was purified from human RBCs obtained from Innovative Research (Novi, MI), following the procedure of Geraci et al.¹² Hb was stored in an aqueous solution at –80 °C for later usage. Prior to use, Hb was passed through Sephadex G-25 (GE Healthcare) chromatography gel, equilibrated with the appropriate buffer, either 100 mM *N*-2-(hydroxyethyl)piperazine-*N'*-2-ethanesulfonic acid (HEPES) or phosphate-buffered saline (PBS).

All buffered solutions also contained 0.1 M KCl and 0.1 mM diethylenetriaminepentaacetic acid. In light of the well-known pH artifacts associated with the freezing of a sodium phosphate buffer,¹³ we utilize the HEPES buffer primarily and, to illuminate buffer effects, potassium PBS.

metHb was prepared by the treatment of Hb with potassium ferricyanide, followed by G-25 filtration to remove excess oxidant. To prepare metHb/NO₂[–], aliquots of buffered (HEPES or PBS) aqueous solutions of NaNO₂ were added to metHb solutions with nitrite at a 20-fold excess over heme.

Fe^{II}NO/Fe^{III}NO₂[–]-Hb Hybrids. To probe for subunit specificity of the nitrite/metHb complexes, reactions were carried out with metHb/nitrosyl-Hb hybrids, which were prepared in two distinct ways. First, to obtain Hb with preferentially oxidized β subunits (and nitrosylated α subunits), Hb was initially incubated with sodium nitrite and sodium dithionite under anaerobic conditions to generate Hb(NO)₄; the solution was then subjected to gel filtration to remove any excess reagents. The resulting Hb(NO)₄ solution was then exposed to room air for approximately 7 h at 20 °C. This procedure results in the preferential oxidation of β-Fe^{II}NO to Fe^{III}.² The concentration of metHb present was assayed by UV–vis spectroscopy, while the subunit specificity was determined by EPR spectroscopy.² A concentrated NaNO₂ solution was then added to form the α-Fe^{II}NO/β-Fe^{III}NO₂[–] hybrid complexes.

Complementary Hb hybrids, with oxidized α subunits and nitrosylated β subunits, were prepared by reductive nitrosylation of metHb with a [NO]/[heme] ratio of 0.9:1 using diethylamine NONOate (DEANO; Cayman Chemical, Ann Arbor, MI) as the NO donor.² The reaction progress was monitored using UV–vis spectroscopy. Following reductive nitrosylation, concentrated NaNO₂ was added in a molar excess over the remaining Fe^{III}, to furnish α-Fe^{III}NO₂[–]/β-Fe^{II}NO hybrid complexes.

SNO-Hb's. SNO-Hb was prepared by reacting oxygenated Hb in a pH 9.2 borate buffer with acidified nitrite. Following incubation, the SNO-Hb solution was passed through a G-25 column equilibrated with a pH 7.4 HEPES buffer. The SNO-Hb yield was determined by Greiss and Saville assays, as described previously.¹⁴ SNO-Hb was then oxidized with potassium ferricyanide with subsequent G-25 filtration. Concentrated NaNO₂ was added in a molar excess, as determined by UV–vis spectroscopy, to furnish SNO-metHb/nitrite.

D₂O Solutions. To prepare a solution of metHb/NO₂[–] in D₂O, Hb was first treated with potassium ferricyanide, followed by G-25 filtration, and then concentrated using a Microcon 30 centrifugal filter (Millipore, Billerica, MA). The protein was reconstituted in 1:10 (v.v) HEPES-buffered deuterium oxide (Cambridge Isotope Laboratories Inc., Cambridge, MA). The pD of the solution was set to 7.4, as determined with a glass electrode using pH + 0.4.¹⁵

EPR Spectroscopy. X-band EPR data were collected on a Varian E-109 spectrometer modified with a National Instruments computer interface for data collection and field control. For spectra obtained at liquid-helium temperatures, a Heli-Tran LTD-3-110 (Air Products and Chemicals Inc., Allentown, PA) liquid-helium transfer system and dewar was employed. For X-band spectra obtained at 100 K and above, sample cooling was provided by a flow-through setup utilizing a constant stream of liquid-nitrogen-cooled gas. S-band EPR data collection was conducted on a Bruker EMX spectrometer with an ER061ST microwave bridge and a flexline cavity assembly. Liquid-helium temperatures were achieved through use of an Oxford Instruments CF-905 cryostat. Detailed simulation of experimental

(4) Angelo, R. M.; Singel, D. J.; Stamler, J. S. *Proc. Natl. Acad. Sci. U.S.A.* **2006**, *103*, 8366–8371.

(5) Luchsinger, B. P.; Rich, E. N.; Yan, Y.; Williams, E. M.; Stamler, J. S.; Singel, D. J. *J. Inorg. Biochem.* **2005**, *99*, 912–921.

(6) Basu, S.; Grubina, R.; Huang, J.; Conradi, J.; Huang, Z.; Jeffers, A.; Jiang, A.; He, X.; Azarov, I.; Seibert, R.; Mehta, A.; Patel, R.; King, S. B.; Hogg, N.; Ghosh, A.; Gladwin, M. T.; Kim-Shapiro, D. B. *Nat. Chem. Biol.* **2007**, *3*, 785–794.

(7) Rodkey, F. L. *Clin. Chem.* **1976**, *22*, 1986–1990.

(8) Young, L. J.; Siegel, L. M. *Biochemistry* **1988**, *27*, 2790–2800.

(9) Peisach, J.; Blumberg, W. E.; Ogawa, S.; Rachmilewitz, E. A.; Oltzik, R. *J. Biol. Chem.* **1971**, *246*, 3342–55.

(10) Schwab, D. E.; Stamler, J. S.; Singel, D. J. *Nat. Chem. Biol.* **2009**, *5*, 366–366.

(11) Yi, J.; Safo, M. K.; Richter-Addo, G. B. *Biochemistry* **2008**, *47*, 8247–8249.

(12) Geraci, G.; Parkhurst, L. J.; Gibson, Q. H. *J. Biol. Chem.* **1969**, *244*, 4664–4667.

(13) Williams-Smith, D. L.; Bray, R. C.; Barber, M. J.; Tsopanakis, A. D.; Vincent, S. P. *Biochem. J.* **1977**, *167*, 593–600.

(14) Gow, A. J.; Luchsinger, B. P.; Pawloski, J. R.; Singel, D. J.; Stamler, J. S. *Proc. Natl. Acad. Sci. U.S.A.* **1999**, *96*, 9027–9032.

(15) Glasoe, P. K.; Long, F. A. *J. Phys. Chem.* **1960**, *64*, 188–190.

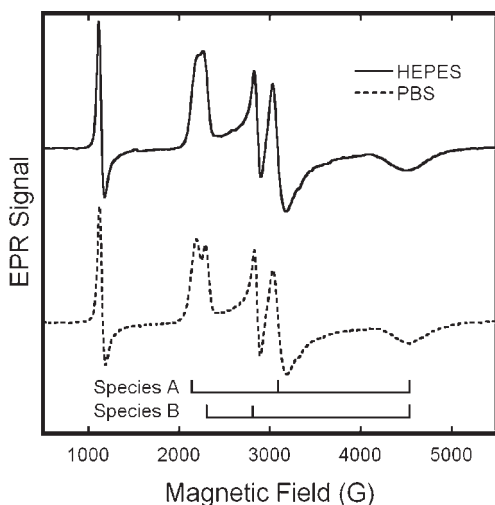


Figure 1. X-band EPR spectra of solutions of metHb/NO₂⁻ in HEPES (—) or PBS (---) buffer at 20 K. The samples included metHb at 0.5 M and a 20-fold molar excess (per heme) of NaNO₂; the buffer concentration was 0.1 M and the pH 7.4. EPR spectra were obtained with the following spectrometer parameter values: 0.5 s time constant, 5 G modulation amplitude, 16.67 G/s sweep rate, 5 mW microwave power, and 9.24 GHz microwave frequency.

EPR data was conducted using the program *EasySpin*.¹⁶ Observed alterations in the quality of the fit, with changes in the parameter values, were used as a guide to the precision of the determination of the values. Simulated spectra were then used as basis spectra for least-squares decomposition of multicomponent EPR spectra, using a fitting program similar to that described by us previously.²

UV–Vis Spectroscopy. UV–vis spectra were collected using a Cary 300 spectrometer. Least-squares fitting of spectra² was used to determine the concentration of UV–vis-detectable heme species.

Results

Doublet Structure. Low-temperature EPR spectra of our neutral-pH, neat metHb preparations consist, generally, of spectral contributions from three distinct chemical species: (1) high-spin aquo-metHb; (2) low-spin hydroxymetHb; (3) an additional low-spin species that has been proposed to result from coordination of a nitrogen atom of the distal histidine as the sixth heme iron ligand.¹⁷ Detailed simulations of our experimental metHb spectra (not shown) agree well with the results of Svistunenko and co-workers, with regard to both the spectral properties and the relative amounts of each of the three species.¹⁷

The addition of excess sodium nitrite to neutral-pH metHb solutions results in the substantial replacement of the metHb EPR signals with new features in the region associated with low-spin Fe^{III} hemichromes. In the X-band EPR spectra shown in Figure 1, these new features entail a broad, high-field feature at ~4500 G, a closely spaced doublet, low-field feature at ~2200 G, and a well-resolved doublet, intermediate-field feature at ~3000 G. The sharp feature at ~1100 G is from the remaining aquo-metHb. As evidenced in Figure 1, the resolution of the low-field doublet exhibits some sensitivity to the nature of the buffer.

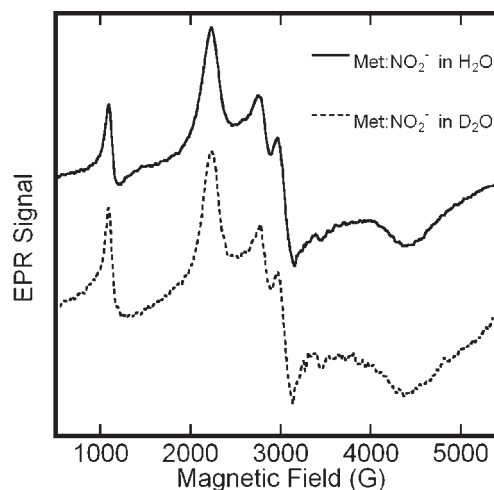


Figure 2. EPR spectra of solutions of metHb/NO₂⁻ in H₂O and D₂O in boiling nitrogen (76 K). The protein concentration was 0.5 M in the H₂O sample and 0.4 M in the D₂O sample. Both samples contained a 20-fold molar excess (per heme) of NaNO₂, buffered at an effective pH of 7.4 in HEPES. Spectral amplitudes were corrected for differences in the concentration. Both EPR spectra were recorded at 9.12 GHz with a 16.67 G/s sweep rate, a 0.5 s time constant, a 5 G modulation amplitude, and 10 mW of microwave power.

It is better resolved, with sharper component lines and minor changes in line position in PBS (Figure 1, bottom). Nevertheless, the fundamental features are the same; intrinsic buffer effects represent a modest perturbation, in contrast to suggestions made by others.¹⁸

We considered two alternative hypotheses for the origin of this structure: (1) the splittings reflect a hyperfine structure, or (2) they reflect the overlap of the unstructured spectra of two low-spin hemichromes with a slight difference in their high and intermediate *g* values. To distinguish between these possibilities, we undertook two experiments. First, we obtained the EPR spectrum of isotopically labeled metHb/NO₂⁻ samples. Given the size of the splittings, the coupling would most likely involve a hydrogen atom whose 1s orbital has substantial overlap with iron *t*_{2g} orbitals, perhaps a proton associated with the nitrite ligand. To test this possibility, we obtained the EPR spectrum of the metHb/nitrite complex in a HEPES buffer in D₂O (Figure 2). The spectra are essentially identical with the ones obtained in H₂O; in particular, the splitting of the two central features is unchanged. [Analogous results were obtained in complexes formed with ¹⁵N-nitrite (data not shown).] To validate this result, we compared EPR spectra obtained at X band with spectra obtained at S band (3.9 GHz). The S-band spectrum (Figure 3) exhibits splittings in both the low- and intermediate-field features that scale in proportion to a reduction in the microwave frequency from the X band to the S band. If the observed splitting had originated from a hyperfine interaction, then the splitting would be expected to remain constant over this microwave frequency range. Collectively, the multifrequency EPR and the isotopic labeling experiments indicate that the EPR spectrum of metHb/NO₂ is caused by the presence of

(16) Stoll, S.; Schweiger, A. *J. Magn. Reson.* **2006**, *178*, 42–55.

(17) Svistunenko, D. A.; Sharpe, M. A.; Nicholls, P.; Blenkinsop, C.; Davies, N. A.; Dunne, J.; Wilson, M. T.; Cooper, C. E. *Biochem. J.* **2000**, *351* (3), 595–605.

(18) Goetz, B. I.; Wang, P.; Shields, H. W.; Basu, S.; Grubina, R.; Huang, J.; Conradie, J.; Huang, Z.; Jeffers, A.; Jiang, A.; He, X.; Azarov, I.; Seibert, R.; Mehta, A.; Patel, R.; King, S. B.; Ghosh, A.; Hogg, N.; Gladwin, M. T.; Kim-Shapiro, D. B. *Nat. Chem. Biol.* **2009**, *5*, 367–367.

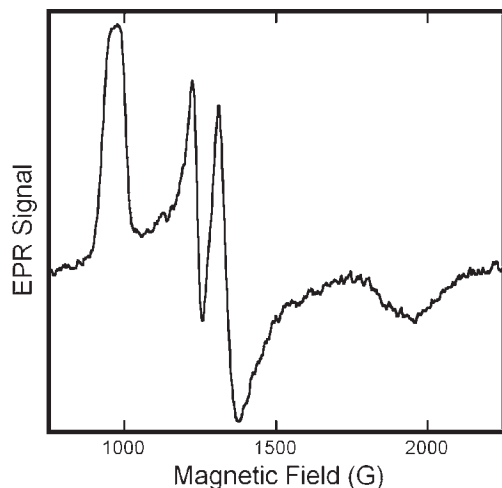


Figure 3. S-band EPR spectrum of solutions of metHb/NO₂⁻. The sample was prepared in a pH 7.4 HEPES buffer with a protein concentration of 0.75 M and a 20-fold molar excess (per heme) of NaNO₂. The spectrum was obtained with the sample at ~40 K and at a frequency of 3.98 GHz, with a sweep rate of 17.88 G/s, a time constant of 0.328 s, a 5 G modulation amplitude, and 9.7 mW microwave power.

two distinct species. Accordingly, returning to the upper spectrum of Figure 1, we determine the metHb/nitrite EPR spectra to have principal g values of (3.006, 2.887), (2.299, 2.129), and 1.45 (HEPES, 20 K). The assignment of the pairs of values in parentheses to unique species is not obvious from the spectra but can be made on the basis of observations of the differential effects of the pH on the size of the components of each doublet (vide infra).

pH Dependence. As illustrated in Figure 4, the relative intensities of the subcomponents of each doublet feature in the EPR spectra of metHb/NO₂⁻ exhibit notable variations with the pH over the range of 5 to 10. As the pH increases, the intensity of the feature at $g \approx 2.9$ increases relative to that at $g \approx 3.0$. This change in the intensity is mirrored by the increase in the intensity of the $g \approx 2.3$ feature relative to the $g \approx 2.1$ feature. This concerted variation allows for the assignment of features to two species, metHb/NO₂⁻ A and B, with g values (g_x, g_y, g_z) of (3.018, 2.122, 1.45) and (2.870, 2.304, 1.45) (PBS, 20 K) and thus of (3.006, 2.129, 1.45) and (2.887, 2.299, 1.45) (HEPES, 20 K). This assignment balances the sizes of the g values, consistent with the general rule for hemichrome principal g values that the sum of their squares be ~ 16 .¹⁹

With increases in the pH above 8.3, the relative intensities of the metHb/NO₂⁻ signals decrease, as OH⁻ becomes competitive with NO₂⁻ as a ligand. In the series depicted in Figure 4, for a sample with a 20-fold molar excess of NaNO₂⁻ over heme, metHb/OH⁻ becomes apparent at a pH of ~ 8.3 . At pH 10.0, metHb/OH⁻ accounts for approximately 60% of the detected species.

In addition to changes in complexation, this series of EPR spectra also reveal changes in the positions of certain features in the metHb/NO₂⁻ spectra with pH. The greatest change is sustained by the low-field feature of metHb/NO₂⁻ species A: it appears at $g \approx 3.00$ at pH 5.0, $g \approx 3.02$ at pH 7.4, and $g \approx 3.04$ at pH 10.0. The central feature of

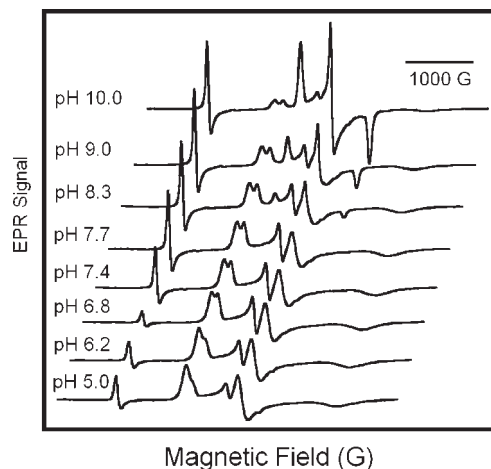


Figure 4. pH dependence of the EPR spectrum of metHb/NO₂⁻. Solutions of metHb in PBS poised at pH values as indicated in the figure and 0.5 mM protein and 40 mM NaNO₂ for all samples. The EPR spectra were recorded at 20 K with a microwave frequency of 9.24 GHz, a 16.67 G/s sweep rate, a 0.5 s time constant, a 5 G modulation amplitude, and 5 mW of microwave power.

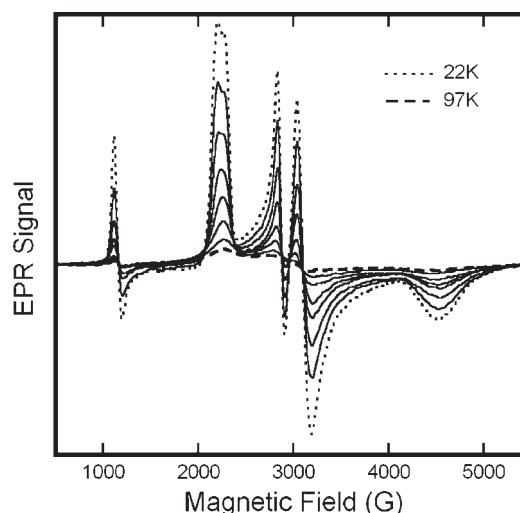


Figure 5. Variable-temperature EPR spectra of solutions of metHb/NO₂⁻ in a HEPES buffer at pH 7.4. The sample included metHb at 0.65 M and a 20-fold molar excess (per heme) of NaNO₂⁻. Spectra were obtained at 22, 32, 43, 54, 65, 76, 86, and 97 K. The EPR spectra were recorded at 9.24 GHz with a 16.67 G/s sweep rate, a 0.5 s time constant, a 5 G modulation amplitude, and 5 mW of microwave power.

species A ($g = 2.12$) also shifts as a function of the pH, although its exact position is difficult to follow because it is masked at higher pH by the metHb/OH⁻ spectrum. Nevertheless, the parallel trend lends further support to our assignment of this feature and the $g = 3.02$ feature to the same species. Changes to metHb/NO₂⁻ B features are more subtle; the low-field feature of species B varies from $g = 2.86$ at pH 5.0 to $g = 2.87$ at pH 10.0. The broad high-field features of both species A and B do not show discernible, pH-dependent changes in position.

Variable-Temperature EPR. The presence of multiple species that are distinguished by EPR in samples of metHb/NO₂⁻ is reminiscent of the behavior of Fe^{II}NO in Hb-(NO)₄. EPR spectra in Hb-(NO)₄ show two different species (axial and rhombic) with, moreover, subunit distinctions that are most clearly illuminated in variable-temperature

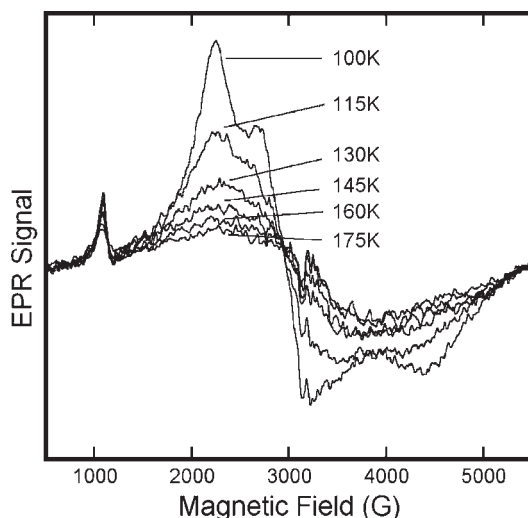


Figure 6. Variable-temperature EPR spectra of solutions of metHb/NO₂⁻ in a HEPES buffer at pH 7.4. The sample included metHb at 0.65 M and a 20-fold molar excess (per heme) of NaNO₂⁻. Spectra were obtained at the indicated temperatures in the range of 100–175 K. EPR spectra were recorded at 9.1 GHz with a 16.67 G/s sweep rate, a 0.5 s time constant, a 5 G modulation amplitude, and 10 mW of microwave power.

EPR studies.^{20,21} In light of this precedent, we undertook variable-temperature EPR studies of metHb/NO₂⁻. Exemplary spectra are shown in Figures 5 and 6.

At temperatures below 20 K, the metHb/NO₂⁻ spectrum is readily saturated and, absent of sufficient care, subject to line-shape and intensity distortion, as has been recently realized by others.¹⁸ Spectra are obtained with facility in the temperature range of 20–100 K and display only very subtle changes in the position and shape of spectral features. The separate components of the low-field feature remain resolved until the temperature is raised to ~54 K, while the central doublet remains resolved until the temperature exceeds ~100 K. There appears to be little, if any, net interconversion between the two species, in contrast to the spectrum of Hb(NO)₄, which over a similar temperature range shows striking changes reflective of a temperature-dependent equilibrium between the axial and rhombic species.²¹ This effect was first noted in the EPR spectrum of Fe^{II}NO myoglobin by Morse and Chan.²² As illustrated in Figure 6, once the sample temperature exceeds 115 K, there appears to be sufficiently rapid and unrestricted motion of the nitrite ligand, in which the spectra of both of the metHb/NO₂⁻ species no longer exhibit *g* anisotropy.

In light of the motional averaging that ensues at cryogenic temperatures, the apparent lack of a temperature-dependent interconversion between the metHb/NO₂⁻ A and B species at lower temperatures is intriguing. It is possible that the temperature dependence of an equilibrium constant between the A and B species is small enough (e.g., if A and B were isoenthalpic) that no temperature dependence of the partitioning into A and B spectra is observed. Alternatively, it may be the case that the motion that the ligand undergoes cannot support

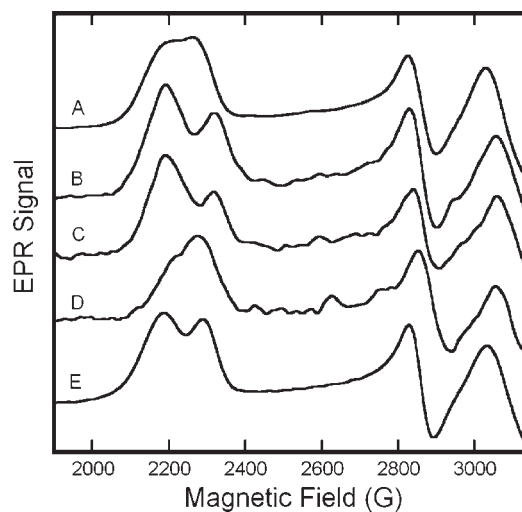


Figure 7. EPR spectra of Fe^{II}NO/Fe^{III}NO₂⁻ hybrids and related Hb's. For detail, only the variable, low-field portion of the spectrum is shown: (A) metHb/NO₂⁻ in HEPES, pH 7.4; (B) β-Fe^{II}NO/α-Fe^{III}NO₂⁻ in HEPES, pH 7.4; (C) SNO-metHb/NO₂⁻ in HEPES, pH 7.4; (D) α-Fe^{II}NO/β-Fe^{III}NO₂⁻ hybrid in HEPES, pH 7.4; (E) metHb/NO₂⁻ in PBS, pH 7.4. All spectra were recorded at 20 K with a frequency of 9.24 GHz, a 0.5 s time constant, and a sweep rate of 16.67 G/s. For spectra A and E, the modulation amplitude was 5 G and the microwave power was 5 mW. Spectra B–D were recorded with a 1 G modulation amplitude and 10 mW microwave power.

species interconversion. This possibility is very difficult to reconcile with a conjecture that species A and B entail structural or linkage isomers; rather, it strongly suggests that A and B reflect differences in nitrite binding between the α and β subunits of Hb, in which case motion leading to spectral averaging could occur entirely within a given subunit's heme pocket, without intersubunit ligand exchange. However, if species A and B are each associated with a particular subunit, equal populations of each are expected in the presence of putatively saturating nitrite. Detailed simulation of the spectra revealed that the A:B ratio is not 1:1 and thus suggests that binding modes entail greater complexity than simple subunit inequalities.

Hb Hybrids. In an effort to further illuminate possible subunit differences in nitrite binding to Hb, we prepared hybrids of the form α-Fe^{II}NO/β-Fe^{III}Hb and β-Fe^{II}NO/α-Fe^{III}Hb and examined the EPR spectra of their nitrite complexes. In these experiments, the balance between ferrous nitrosyl and metHb species was assayed by UV–vis spectroscopy, while the subunit populations were monitored by examination of their Fe^{II}NO EPR spectra.²

A first class of samples was prepared by reductive nitrosylation with limiting NO.² An exemplary preparation, the spectra of which are shown in Figure 7B, was analyzed as 30% Fe^{II}NO and 70% Fe^{III}, with Fe^{III} distributed as >66% α and <33% β. A second class of samples (Figure 7D) was created through partial autoxidation of Hb(NO)₄, which resulted in 56% Fe^{II}NO and 44% Fe^{III}, 2% of which was α-Fe^{III} and the remaining 98% β-Fe^{III}. To each hybrid was then added NaNO₂ to a 20-fold molar excess over the ferric heme present.

As compared to the spectrum of the nitrite complex of the standard metHb (Figure 7A), the spectrum of the hybrid with excess α-Fe^{III} (Figure 7B) exhibited a reduction in the intensity of the B component of the low-field feature (*g* ≈ 2.89), as well as a shift of that component to a

(20) Flores, M.; Wajnberg, E.; Bemski, G. *Biophys. J.* **1997**, *73*, 3225–3229.

(21) Huttermann, J.; Burgard, C.; Kappl, R. *J. Chem. Soc., Faraday Trans.* **1994**, *90*, 3077–3087.

(22) Morse, R. H.; Chan, S. I. *J. Biol. Chem.* **1980**, *255*, 7876–7882.

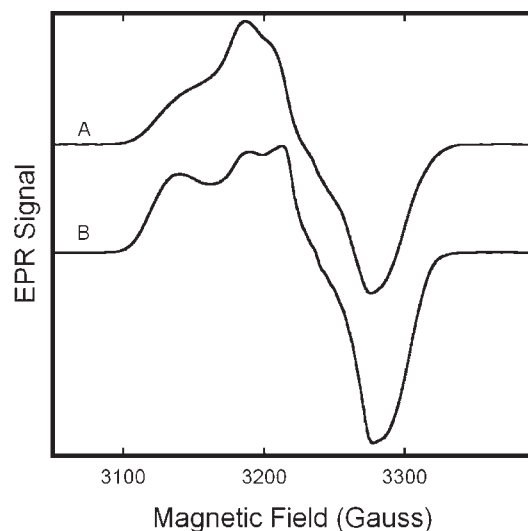


Figure 8. EPR spectra of $\text{Fe}^{\text{II}}\text{NO}$ of $\text{Fe}^{\text{II}}\text{NO}/\text{Fe}^{\text{III}}\text{NO}_2^-$ hybrid Hb's. Only the central region of the spectrum, featuring the ferrous nitrosyl EPR signal, is shown: (A) $\beta\text{-Fe}^{\text{II}}\text{NO}/\alpha\text{-Fe}^{\text{III}}\text{NO}_2^-$, as in Figure 6B; (B) $\alpha\text{-Fe}^{\text{II}}\text{NO}/\beta\text{-Fe}^{\text{III}}\text{NO}_2^-$ hybrid, as in Figure 6D. Spectra were obtained with the sample in boiling nitrogen (76 K), at a microwave frequency of 9.12 GHz, 10 mW microwave power, a 5 G modulation amplitude, a sweep rate of 3.33 G/s, and a time constant of 0.128 s.

slightly higher field ($g \approx 2.85$). The ratio of species A to B was 3.2:1. In the hybrid with excess $\beta\text{-Fe}^{\text{III}}$ (Figure 7D), the position of the two low-field features remains constant, but the $g = 3.006$ feature displays a reduction in the intensity compared to normal $\text{metHb}/\text{NO}_2^-$. The A/B ratio was determined to be 0.8:1. Comparison of the central features is impeded by the much more intense $\text{Fe}^{\text{II}}\text{NO}$ signal (which begins to exhibit an appreciable intensity at ~ 3150 G). Exemplary $\text{Fe}^{\text{II}}\text{NO}$ spectra of the hybrids are shown in Figure 8.

The spectroscopic results on these hybrid experiments are intriguing on multiple levels. First, because the shift of $g \approx 2.89$ to $g \approx 2.85$ was only observed in hybrids prepared through reductive nitrosylation, we hypothesized that the shift might be caused by S-nitrosylation of the $\beta\text{-Cys93}$ thiol, a known product of this reaction.² To test this notion, we prepared an authentic SNO-metHb/ NO_2^- complex. The EPR spectrum of this species, shown in Figure 7C, manifests a perturbation of the $g \approx 2.89$ feature similar to that of the hybrid prepared by reductive nitrosylation. Because S-nitrosylation occurs solely on the β subunit, species B must be associated with $\beta\text{-Fe}/\text{NO}_2^-$. However, the A/B ratios of the two hybrids reveal the simple $\alpha = \text{A}$ and $\beta = \text{B}$ assignment to be inadequate. [In the oxidized $\text{Hb}(\text{NO})_4$ hybrid, the α/β Fe^{III} ratio was 1:49, yet the A/B ratio was 0.8:1; the hybrid prepared through reductive nitrosylation had an α/β Fe^{III} ratio of 2:1 and an A/B ratio of 3.2:1.] The simplest explanation consistent with our results is that $\alpha\text{-Fe}^{\text{III}}\text{NO}_2^-$ is found as species A only, while $\beta\text{-Fe}^{\text{III}}\text{NO}_2^-$ can assume a conformation/linkage consistent with either spectrum A or B.

Affinity. Dissociation constants (K_d) of $\text{metHb}/\text{NO}_2^-$ were determined by means of the Hill analysis²³ detailed in Figure 9. In these experiments, we examined samples in both PBS and HEPES and added nitrite at molar equivalence and in 5-, 10-, and 20-fold excess over met-heme.

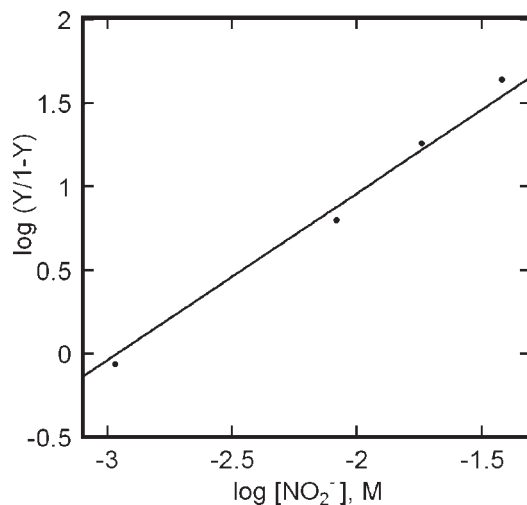


Figure 9. Exemplary Hill plot summarizing the titration of metHb with NaNO_2 . The species concentrations used in the plot were obtained from a detailed simulation of experimental EPR spectra. For the particular trial depicted in this plot, the protein concentration was 0.5 mM (pH 7.4 HEPES), with NaNO_2 at, alternatively, 1-, 5-, 10-, and 20-fold excess over heme. Supporting data are provided in the Supporting Information.

The analysis utilized concentrations determined by UV-vis, with differentiation of the Fe^{III} products and reactants being determined by EPR spectroscopy. The assayed concentrations confirmed mass balance of protein before and after the addition of nitrite; no evidence for the formation of EPR-silent products was observed. The concentration of nitrite in solution was calculated as the original nitrite added less $\text{metHb}/\text{NO}_2^-$ formed, as was done by others.^{6,18,24} The absence of change in the $\text{metHb}/\text{NO}_2^-$ EPR spectrum over several hours suggests that there is no, or limited, consumption of nitrite under our reaction conditions, supporting the method employed to estimate the nitrite concentration. The slope of the Hill plot reflects the absence of cooperativity in ligand binding and affords values for K_d of $\text{metHb}/\text{NO}_2^-$ of 1.24 ± 0.5 mM in HEPES, pH 7.4, and 1.68 ± 0.4 mM in potassium PBS, pH 7.4.

A cursory examination of the peak heights of aquo-metHb versus $\text{metHb}/\text{NO}_2^-$ reveals a pH dependence of the affinity of metHb for nitrite. The affinity of metHb for nitrite is greatest at pH 6.8, though the change in the affinity with the pH is less dramatic than the sharp nature of the $g = 6$ aquo-metHb would lead one to believe. Additionally, having obtained the relative concentrations of the various components in experimental spectra (Figure 4), we determined the $\text{p}K_a$ of the water ligand to be 8.15 at pH 8.3, which is in good agreement with the values determined previously.^{25,26}

Discussion

The EPR measurements of $\text{metHb}/\text{NO}_2^-$ presented here indicate that the addition of NaNO_2 to metHb results in the formation of two distinct heme- $\text{Fe}^{\text{III}}\text{NO}_2^-$ species. EPR measurements at multiple frequencies and measurements in

(23) Hill, A. V. *J. Physiol.* 40, i-vii.

(24) Goetz, B. I.; Shields, H. W.; Basu, S.; Wang, P.; King, S. B.; Hogg, N.; Gladwin, M. T.; Kim-Shapiro, D. B. *Nitric Oxide* 2010, 22, 149-154.

(25) Coryell, C. D.; Stitt, F.; Pauling, L. *J. Am. Chem. Soc.* 1937, 59, 633-642.

(26) Okonjo, K. O.; Vega-Catalan, F. J. *Eur. J. Biochem.* 1987, 169, 413-416.

D₂O rule out the assignment of this splitting as a hyperfine structure. Systematic changes in the EPR spectra with pH enable the assignment of each component of the doublet features to the spectra of two species. Thus, we conclude that the EPR spectrum of metHb/NO₂⁻ is a composite of two species with *g* values of 3.018, 2.122, 1.45 and 2.870, 2.304, 1.45 at pH 7.4 in PBS and 3.006, 2.129, 1.45 and 2.887, 2.299, 1.45 at pH 7.4 in a HEPES buffer. On the basis of EPR studies of Fe^{III}NO₂⁻/Fe^{II}NO hybrids, we conjecture that one of the species is present in both the α and β subunits, while the other is exclusive to the β subunit. EPR experiments on hybrids also led to the discovery of an effect of S-nitrosylation on the β -subunit Fe^{III}NO₂⁻ EPR spectrum.

In their pioneering EPR studies of hemichromes, Blumberg and Peisach²⁷ used *g* values to categorize low-spin Fe^{III} heme proteins and model complexes according to the relative sizes of the tetragonal and rhombic ligand-field components that they imply. Complexes with different types of axial ligands lie in distinct neighborhoods, when mapped with their ligand-field parameters as coordinates. Both sets of *g* values reported here for metHb/NO₂⁻ fall into the region associated with B-type hemichromes (since termed type II hemichromes¹⁹). This type of hemichrome typically has an Fe^{III}-N bond, such as the imidazole nitrogen atom of the eponymous cytochrome *b*. Characterization as a B-type hemichrome naturally suggests that nitrite coordination to metHb assumes a *N*-nitro, rather than a *O*-nitrito, binding mode, or binds through an atom with electronegativity similar to that of an imidazole nitrogen atom. The recent crystallographic studies of Richter-Addo and co-workers,¹¹ however, reveal *O*-nitrito rather than *N*-nitro coordination and, moreover, revealed the presence of distinct nitrito conformers in the α versus β subunits of metHb/NO₂⁻. The crystallographic and EPR results seem difficult to reconcile. Such discrepancies between solution and crystallographic studies, however, are not without precedent in Hb. In particular, EPR studies of Hb(NO)₄ show marked differences in the *g* values obtained in single-crystal versus frozen-solution EPR samples.^{28,29} Density functional theory calculations presented by Basu and co-workers found *N*-nitro coordination to be about 7 kcal/mol more stable than *O*-nitrito coordination; calculations of the *g* values for the different species may be very illuminating.⁶

Combining the information gained from the variable pH and the hybrid data, assignment of the two metHb/NO₂⁻ species can be proposed. At pH 5, the ratio of species A to B is 7:1 and the two metHb/NO₂⁻ species account for >98% of the metHb species detected, ruling out the assignment of one species to the α subunit and the other species to the β subunit. The spectrum of the SNO-metHb/NO₂⁻ hybrid does link the species B spectrum to the β subunit. Yet, the spectrum of the α -Fe^{II}NO/ β -Fe^{III} hybrid Hb demonstrates that the β subunit can assume conformation of both species A and B, while the α -Fe^{III}/ β -Fe^{II}NO hybrid Hb seems to indicate that the α subunit is only found in the species A form.

The pH dependence of the ratio of the two species suggests a possible origin of the two species. The distal pocket, the site of ligand binding, is larger in the α subunit than in the

β subunit.²¹ Moreover, the distal histidine of the β subunit (β His63) has been shown to swing out of the distal pocket,³⁰ creating more space in the distal pocket and alleviating steric interference with ligands, as was originally suggested by Perutz.^{31,32} This distal histidine rotation is pH-dependent³⁰ and has been reported in a variety of heme proteins.^{33–37} Furthermore, these conformational changes of the distal histidine and pocket are limited to the β subunit,^{30,38} consistent with our results, which indicate that only the β subunit can interconvert between species A and B.

In Figure 4, the relative percentage of species A increases as the pH decreases. Concomitant with this increase is the decrease in the relative percentage of species B, while all other species remain constant, demonstrating the conversion of species B to species A as the pH decreases. The pH-dependent conversion between metHb/NO₂⁻ species is consistent with the pH-dependent rotation of the distal histidine of the β subunit. The movement of the distal histidine opens the distal pocket, allowing nitrite to assume the same conformation as that in the larger α -heme distal pocket, species A.

Movement of the distal histidine would also affect the affinity of metHb for nitrite. At higher pH, the position of the distal histidine of the β -heme sterically hinders ligand binding.^{30,32} Additionally, at high pH, nitrite must compete with hydroxide for metHb, with the more compact hydroxide having easier access to the heme pocket. As the pH decreases and the distal histidine swings out of the heme pocket, ligand binding is enhanced by the additional space created, allowing the β subunits to assume the most energetically favorable conformation. The modest decrease in the affinity below pH 6.8 could possibly result from continued rotation of the distal histidine, especially if species A is stabilized by a hydrogen bond from the imidazole nitrogen atom. Additionally, the p*K*_a of nitrite (3.16 at 298 K³⁹), in conjunction with the reduction of the pH that occurs upon freezing of the PBS buffer,^{13,40} could result in a substantial portion of nitrite being protonated in the pH 5.0 and 6.2 metHb/NO₂⁻ samples, causing an apparent reduction in the metHb affinity for nitrite.

Hb is known to be a robust protein, resisting denaturation over a wide pH range. Hollecher and Buckley demonstrated the efficacy of EPR spectroscopy in measurements of metHb over the pH range from 3 to 12.⁴¹ Others have shown that acid-induced denaturation occurs below pH 4⁴² and that

(30) Jenkins, J. D.; Musayev, F. N.; Danso-Danquah, R.; Abraham, D. J.; Safo, M. K. *Acta Crystallogr., Sect. D: Biol. Crystallogr.* **2009**, *65*, 41–48.

(31) Perutz, M. F. *Nature* **1970**, *228*, 726–739.

(32) Perutz, M. F.; Wilkinson, A. J.; Paoli, M.; Dodson, G. G. *Annu. Rev. Biophys. Biomol. Struct.* **1998**, *27*, 1–34.

(33) Akiyama, K.; Fukuda, M.; Kobayashi, N.; Matsuoka, A.; Shikama, K. *Biochim. Biophys. Acta* **1994**, *1208*, 306–309.

(34) Geibel, J.; Chang, C. K.; Traylor, T. G. *J. Am. Chem. Soc.* **1975**, *97*, 5924–5926.

(35) Tian, W. D.; Sage, J. T.; Champion, P. M. *J. Mol. Biol.* **1993**, *233*, 155–166.

(36) Vallone, B.; Nienhaus, K.; Matthes, A.; Brunori, M.; Nienhaus, G. U. *Proc. Natl. Acad. Sci. U.S.A.* **2004**, *101*, 17351–17356.

(37) Kamimura, S.; Matsuoka, A.; Imai, K.; Shikama, K. *Eur. J. Biochem.* **2003**, *270*, 1424–1433.

(38) Tsuruga, M.; Matsuoka, A.; Hachimori, A.; Sugawara, Y.; Shikama, K. *J. Biol. Chem.* **1998**, *273*, 8607–8615.

(39) da Silva, G.; Kennedy, E. M.; Dlugogorski, B. Z. *J. Phys. Chem. A* **2006**, *110*, 11371–11376.

(40) Orii, Y.; Morita, M. *J. Biochem.* **1977**, *812*, 163–168.

(41) Hollecher, T. C.; Buckley, L. M. *J. Biol. Chem.* **1966**, *241*, 2976–2980.

(42) Munoz, G.; de Juan, A. *Anal. Chim. Acta* **2007**, *595*, 198–208.

(27) Blumberg, W.; Peisach, J. *Adv. Chem. Ser.* **1971**, *100*, 271–291.

(28) Dickinson, L. C.; Chien, J. C. W. *Biochem. Biophys. Res. Commun.* **1974**, *59*, 1292–1297.

(29) Doetschman, D. C.; Utterback, S. G. *J. Am. Chem. Soc.* **1981**, *103*, 2847–2852.

alkaline denaturation occurs above pH 11.⁴³ Using a pH range similar to ours, Svistunenko et al. conducted an EPR investigation of the pH dependence of metHb hemichrome species, noting that all species detected were also present in whole blood.¹⁷ Moreover, the modest changes that we observe in the metHb/NO₂⁻ EPR spectrum (Figure 4) over the pH range employed demonstrate the absence of any protein unfolding that would abrogate the conclusions drawn.

Additionally, we reiterate the weak binding of nitrite to metHb, with K_d of metHb/NO₂⁻ in the millimolar range in both HEPES and PBS buffers. The dissociation constants of metHb/NO₂⁻ presented here are calculated from direct EPR measurements of the various Hb species: aquo-metHb, hydroxy-metHb, and metHb/NO₂⁻, in contrast to the work of Basu et al., in which only aquo-metHb was measured. Our approach allows a check for mass balance and a clear demonstration that the metHb/NO₂⁻ species detected by EPR account for all heme products formed during the reaction. With this check on the sufficiency of the analysis, we obtain dissociation constants that are more reliable than those obtained indirectly⁶ and that are in good agreement with the previously reported optical data.^{7,44}

We also note that the UV-vis data of Basu et al.,⁶ which were obtained to monitor the progress of the reaction of deoxyHb with nitrite, provide an alternative means to estimate the nitrite dissociation constant. In experiments with excess nitrite (for example, Figure 1e of Basu et al.⁶), the reaction reaches an end point in which metHb formed is in equilibrium with the excess nitrite. From the observed concentrations of metHb, metHb/NO₂⁻, and the reported nitrite exposure, dissociation constants can be inferred that are 2 orders of magnitude larger than those determined by their EPR measurements.

The discrepancy provokes one additional comment. In their experimental design, the metHb/NO₂⁻ complex was often formed, as noted above, as a *reaction product*. As such, a metHb/NO₂⁻ basis spectrum must certainly be included in the least-squares decomposition of composite UV-vis

spectra and will obviously improve the least-squares fit. This situation, however, does not justify a claim that metHb/NO₂⁻ is a reaction intermediate. Indeed, their reported data make a better case for the intermediacy of Fe^{III}NO because it is observed to improve the least-squares fit only during the reaction and not at its end point (Figure 1f of Basu et al.⁶).

In closing, it is worth noting some pitfalls that can occur in quantitative analyses of EPR spectra in multicomponent systems. First, care must obviously be taken to ensure that the microwave power applied is appropriate to avoid saturation of all spin components and avoid errors in the interpretation of relative intensities. Second, it is of clear importance, when measuring species with broad spectra, that data be collected over the full magnetic field range; broad high-field features are regularly encountered in low-spin Fe^{III}-heme species. If the full spectrum is not measured, substantial errors in quantitation are possible.⁸ Finally, because transition moments differ for spin systems with different spin multiplicities—even for transitions between nominal $m_s \pm 1/2$ spin states—detailed simulation is required to quantify interconversion among such species: relative integrated intensities can be misleading. Thus, although we observed that the addition of NO₂⁻ to metHb resulted in an overall loss of the (integrated) EPR signal, a detailed simulation of the experimental spectra for both high- and low-spin species demonstrated that the number of spins was conserved after nitrite addition.¹⁰ Apart from spectral simulation, this conservation would not be readily apparent and might be mistaken for the formation of an EPR-“silent” species.

Acknowledgment. This work was supported by National Science Foundation Grant MCB 0981228 (to D.J.S.) and National Heart, Lung, and Blood Institute Grant R01 HL421444 (to J.S.S.). Support from the Murdock Charitable Trust for acquisition of the EMX EPR spectrometer is gratefully acknowledged. The authors also thank Dr. Ben Luchsinger for helpful discussions and suggestions throughout this work.

Supporting Information Available: UV-vis and EPR spectra (Figures 1–3). This material is available free of charge via the Internet at <http://pubs.acs.org>.

(43) Haurowitz, F.; Hardin, R. L.; Dicks, M. *J. Phys. Chem.* **1954**, *58*, 103–105.

(44) Smith, R. P. *Biochem. Pharmacol.* **1967**, *16*, 1655–1664.